

Article

Development of Failure Cause–Impact–Duration (CID) Plots for Water Supply and Distribution System Management

Seungyub Lee ¹, Sueyeun Oak ², Donghwi Jung ^{3,*} and Hwandon Jun ⁴

¹ Department of Civil and Environmental Engineering, University of Utah, Salt Lake City, UT 84112, USA

² Research and Development Center, Dohwa Engineering, 438 Samseong-ro, Gangnam-gu, Seoul 06178, Korea

³ Department of Civil Engineering, Keimyung University, Dalgubeol-daero 1095, Dalseo-gu, Daegu 42601, Korea

⁴ Department of Civil Engineering, Seoul National University of Science and Technology, Gongneung-ro 232, Nowon-gu, Seoul 01811, Korea

* Correspondence: donghwiku@gmail.com; Tel.: +82-53-580-5706

Received: 30 July 2019; Accepted: 16 August 2019; Published: 18 August 2019



Abstract: Understanding the impact and duration (consequences) of different component failures (cause) in a water supply and distribution system (WSDS) is a critical task for water utilities to develop effective preparation and response plans. During the last three decades, few efforts have been devoted to developing a visualization tool to display the relationship between the failure cause and its consequences. This study proposes two visualization methods to effectively show the relationship between the two failure entities: A failure cause–impact–duration (CID) plot, and a bubble plot. The former is drawn for an effective snapshot on the range (extent) of failure duration and the impact of different failures, whereas the latter provides failure frequency information. A simple and practical failure classification system is also introduced for producing the two proposed plots effectively. To verify the visualization schemes, we collected records of 331 WSDS component failures that occurred in South Korea between 1980 and 2018. Results showed that (1) the proposed CID plot can serve as a useful tool for identifying most minor and major WSDS failures, and (2) the proposed bubble plot is useful for determining significant component failures with respect to their failure consequences and occurrence likelihoods.

Keywords: water supply and distribution system (WSDS); failure cause; consequences; impact and duration; visualization

1. Introduction

A water supply and distribution system (WSDS) consists of various components (e.g., water treatment plant (WTP), pump station (PS), reservoir, pipes) to deliver the required quantity of water from source to customers with acceptable pressure and water quality [1]. WSDS component failures can result in water service outages, while the impact area and duration differ for each failure event [2–4]. For example, the segment (i.e., a subsection of the system) delineated by the surrounding valves should be closed (segment isolation) during replacement of a broken pipe [5]. A prolonged suspension of a WTP’s operation would cause a service interruption across an entire city area [6]. Generally, the former case is recovered within several hours, whereas the latter case requires several days. On the other hand, component failures of the same type tend to have similar consequences despite individual failures have different timing and location [7,8]. For example, it is difficult that a local distribution pipe failure causes a service interruption for more than two weeks. Because the ultimate goal of water utilities is

to minimize such service interruptions, understanding the impact and duration of different types of failure events is a critical task for developing effective preparation and response action plans [3,9–11].

During the last two decades, some efforts have been devoted to aggregating pipe failure data mainly to demonstrate a failure prediction method. Farmani et al. [12] developed a pipe failure prediction method for long- and mid-term predictions that considered the impact of both static and dynamic factors (physical pipe and temperature-related factors, respectively). In order to test the proposed method, they collected data for 589 pipe failures in a UK city in which 85% of pipes were made of cast iron. Tabesh et al. [13] collected 337 failure records for 80–300 mm pipes for a year to demonstrate their artificial neural network-based pipe failure prediction model. While the aforementioned studies investigated pipe failure records only, a comprehensive WSDS component failure analysis should be performed with historical records of various components' failure (i.e., WTP, PS, reservoir, pipe, etc.).

A number of studies have been conducted in the water quality domain to analyze the causes of failures based on a statistical analysis of historical records. Onyango et al. [14] investigated and classified the causes of pathogenic outbreaks in a WSDS with two potable water reuse schemes (i.e., direct and indirect potable reuse). They adopted an alphanumeric categorization system for failure events that had five possible failure locations and types, in which the numeric codes (1 to 5) indicated the cause of failure (e.g., water source extraction failure, disinfection system failure, distribution system failure, etc.), whereas the alphabetic codes (A to E) represented the types of failure that occurred (e.g., failure due to equipment breakage, failure due to inadequate maintenance, etc.). The outbreaks that occurred in 19 developed countries from 2003 to 2013 were summarized with the codes in a tabular form. In addition, a pie diagram that showed the proportional causes of pathogenic outbreaks was included in [14]: The majority of the outbreaks originated from failures in the management framework and inadequate infrastructure design (codes A and C). However, a more effective visualization method is required to present the relationship between the cause and consequence of failure at a glance (the consequence result was not included in [14]). In addition, it is not clear that the approach in [14] is also a good solution for hydraulic failures in WSDS.

Lindhe et al. [15] suggested classifying WSDS failures mainly into quantity and quality failures. The former describes the condition in which no water is delivered to customers, whereas the latter indicates that the water quality requirement is not met. They proposed a fault tree method for the integrated risk analysis of a WSDS based on a classification system in which customer minutes lost (CML, failure duration measure) was used to check the acceptable level of risk. The risk here can be understood as a means of evaluating hazard or threat arising from possible events or decisions that are out of control [16]. Although the relationship between the causes and consequences (CML, mean failure rate, etc.) was identified in [8] using the results of Monte Carlo simulation of the fault tree, the statistical results were presented only for three sub-systems of the entire WSDS (raw water, treatment, and distribution system). A systematic analysis of component-scale failures based on real data would provide more insight into the causes and consequences of WSDS failures. In addition, failure consequences can be represented not only by the failure duration but also by the failure impact (e.g., the number of people/households impacted), while the two entities are often not perfectly correlated.

In summary, to the best of the authors' knowledge, no study has been performed (1) to collect the impact and duration records of real WSDS failures, (2) to statistically identify the relationship between the two properties and the cause of failures in a comprehensive scheme, and (3) to propose visualization methods to facilitate the investigation results. A proper visualization method should be developed to effectively identify the relationship between failure impact and duration. To that end, this study proposes two visualization methods to effectively depict the relationship between the cause and consequences (failure impact and duration) of WSDS failures: A failure cause–impact–duration (CID) plot and a bubble plot. The visualization tool is a great tool to interact and communicate with the non-professional stakeholders (i.e., policymakers, practitioners, lawyers, etc.) [17]. The former is drawn for an effective snapshot on the ranges (extents) of failure duration and the impact of different failures, whereas the latter provides failure frequency information. A simple and practical failure

classification system is also introduced to produce the two proposed plots effectively. To verify the visualization schemes, we collected the records of 331 WSDS failures (WTP, reservoir, PS, water main, distribution pipe, etc.) that occurred in South Korea between 1980 and 2018.

2. Methodologies

This section provides the details of the proposed failure classification system, failure CID plot, and CID bubble plot.

2.1. Failure Classification

The WSDS failure cause classification system introduced here first classifies “causes” into internal and external triggers (Table 1). Note that WSDS failure here is indicating any incidents that lead to water service interruption. The ultimate cause of an internal trigger originates within the system, e.g., the malfunction of a pumping unit in a WTP or a pipe burst. On the other hand, the cause of an external trigger comes from outside of the system (e.g., natural disasters such as an earthquake, intentional contamination, etc.). Further divided into facility and pipe triggers, internal triggers comprise a total of seven types of WSDS failure triggers: Raw water pumping facility (RWPF), WTP, reservoir (RES), PS, water supply pipe (WSP), distribution main pipe (DMP), and distribution pipe (DP) (Table 1). The first four triggers occur in a WSDS facility that generally occupies a large space in a building structure with associated subcomponents to support its function. Therefore, the failure triggers can be caused by deterioration and malfunction of subcomponents, etc [18,19]. However, the last three are WSDS failure triggered by the pipes that occur in a line-shaped component of a WSDS that delivers water from one location to another. Pipe burst is the most common cause of this kind of failure [18,19]. In this study, external failures are either classified as a water quality failure (WQF) or a natural disaster (ND). Red water (mainly caused by the release of corrosion products from pipes [20]) and turbid water (caused by particles suspended or dissolved in service water) are examples of WQF. Note that the aforementioned WSDS component failures specially by catastrophic disaster events (e.g., the ceasing of a submerged pump station due to typhoon flooding) are classified in the category of ND, and represent the minority of failure cases. This is because a component failure from earthquakes or typhoons should be separately considered with that occurred under normal operating conditions. While the frequency characteristics of the latter tend to follow natural randomness by system internal issues (e.g., natural aging), the former is the secondary failure whose characteristics are controlled by system external forces.

Table 1. WSDS failure classification system proposed in this study.

Level-1 Classification		Level-2 Classification
Internal trigger	Facility failure	Raw water pumping facility (RWPF) Water treatment plant (WTP) Reservoir (RES) Pump station (PS)
	Pipe failure	Water supply pipe (WSP) Distribution main pipe (DMP) Distribution pipe (DP)
External trigger		Water quality failure (WQF) Natural disaster (ND)

2.2. Visualization Methods

This study introduces two 2-dimensional plots (i.e., failure CID plot and bubble plot) to effectively display the relationship between the cause and consequences of WSDS component failures. Water utilities can use and refer to the proposed plots to prepare for and respond to failure conditions. The most significant advantage of the visualization tool is its easiness of communication with the non-professional stakeholders (i.e., policymakers, practitioners, lawyers, etc.) which helps them to

understand the needs of the system to determine investment and financing options for the further planning and management of the WSDS. Successful visualization will provide a useful comparison among the failure triggers and also help to identify the most vulnerable or critical failure trigger that requires close scrutiny. It is worthwhile to highlight that the visualization tool can also support risk analysis related to failure probability, but it is beyond the scope of this study.

This subsection describes the characteristics and steps of the plots. First, WSDS component failure records should be collected from water utilities that include the failure consequence data, i.e., failure impact and duration. Data collection should be limited in the extent to the area of interest. Failure impact data is generally recorded either by the number of households affected by failure (the number of households out of service) or the size of the administrative districts out of service. In the latter case, the number of affected households should be estimated. The failure duration data represents the period of water service outage due to failure (e.g., hours, days). Then, the cause of a failure event is classified with respect to the categorization system in Table 1. Therefore, each failure is coded as one of the nine failures in Table 1.

2.2.1. Failure CID Plot

The proposed failure CID plot is a 2-dimensional plot with the failure duration along the *x*-axis and the failure impact along the *y*-axis (Figure 1). Figure 1 illustrates an example of the CID plot, which is only for demonstration purpose and not drawn with the actual data. The cause of failure is displayed in the middle of a box subplot on the 2-dimensional plot bounded by the minimum and maximum values of the failure duration and impact of each failure classification in Table 1. Note that, while each failure event of the same type (cause) of failure can have different consequences, it is more effective to use such area plots to show the overall range of the consequences of failure. For example, as shown by the light gray box labeled DP in the lower-left corner of Figure 1, the range of failure duration for DP failure is from 1 to 12 h, whereas its impact varies from 10 to approximately 1000 households (small to medium-sized districts). Another form of the CID plot (i.e., ID plot) can be drawn to show the impact and duration of individual failure (cause) in a single plot. Therefore, a total of nine ID plots are produced with identical *x*- and *y*-axis scales for effective comparison.

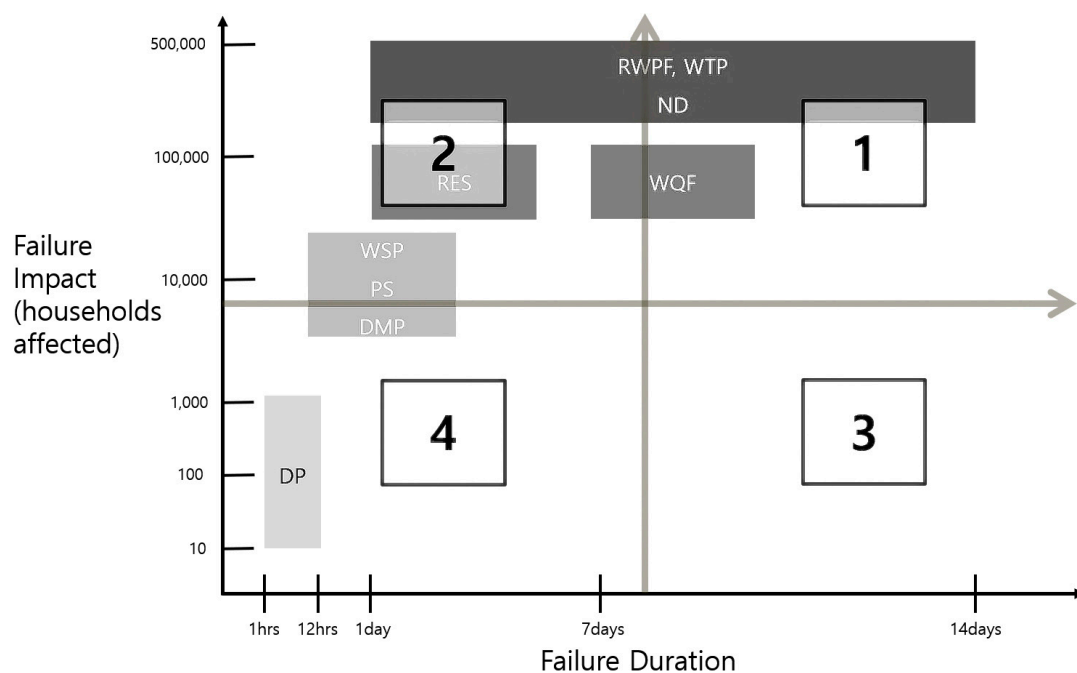


Figure 1. Example of the proposed failure cause-impact-duration (CID) plot.

The proposed CID plot can be divided into four quadrants by setting a threshold for each of the failure durations and impacts beyond which water utilities should adopt system-wide emergency and recovery actions (Figure 1). Quadrant 1 (Q1) in the upper right corner of the CID plot includes the most critical WSDS component failures that have a significant consequence on the system in general with more than one week of service interruption to a number of households greater than 10,000 (at least the majority of a small city is affected) (Figure 1). For example, RWPF failure would cause water service failure to an entire city having a single raw water intake location. In such failures, an emergency interconnection pipe should be operated to receive water from neighboring cities with sufficient resources [7,21]. While the most frequently occurring daily failures (e.g., DP) are located in quadrant 4 (Q4), quadrant 2 (Q2) shows failures with great impact, but that can be recovered from within days. Those positioned in quadrant 3 (Q3) are prolonged failures with a minor impact on the system. In 2010, the breakage of a 150 mm WSP installed under the sea to supply 70 customers living on an island in Korea resulted in a water service outage for 220 h (about 9 d). System-specific thresholds should be determined by the water utility considering the system conditions and management target.

Water utility with a high management standard will have the cross of the threshold lines at the lower-left corner of the CID plot with the largest quadrant area in Q1. On the other hands, a tolerant utility would position the cross at the upper-right corner in the plot with a large Q4 area.

2.2.2. CID Bubble Plot

Multiple plots should be used to capture all failure-characteristic information laid in the historical records. Although the proposed CID plot provides an effective snapshot of the ranges (extent) of failure duration and the impact of different failures, failure frequency information is difficult to incorporate and visualize in a plot. Therefore, we also propose a CID bubble plot in which each failure is drawn as a bubble on the 2-dimensional plot with the same axis as the CID plot, where each bubble has a radius proportional to the frequency of the corresponding failure (Figure 2). For example, based on Figure 2, DMP and DP failures are the most frequently occurring, whereas there are few RWPF failures. The center of the bubble is positioned at either the average or maximum values for failure duration and impact from the corresponding failure in the historical failure records collected which can be expressed as follows:

$$(x_{bubble}, y_{bubble})_j = \begin{cases} \left(\frac{\sum_{i=1}^{n_j} FD_{i,j}}{n_j} \vee \frac{\sum_{i=1}^{n_j} FI_{i,j}}{n_j} \right) \\ \left(\max(FD_{i,j}) \vee \max(FI_{i,j}) \right), \quad i = 1, \dots, n_j \end{cases} \quad (1)$$

where $(x_{bubble}$ and $y_{bubble})_j$ indicate the x and y coordinates of the j th bubble (failure cause of j th categorization in Table 1) in the CID bubble plot; FD_{ij} and FI_{ij} are the failure duration and impact of the j th failure's i th event (e.g., $j = 1$ for RWPF failure in Table 1); n_j is the total number of events of the j th failure recorded. Note that n_j is more likely to be different for different failures in Table 1 and \vee is the "Or" sign.

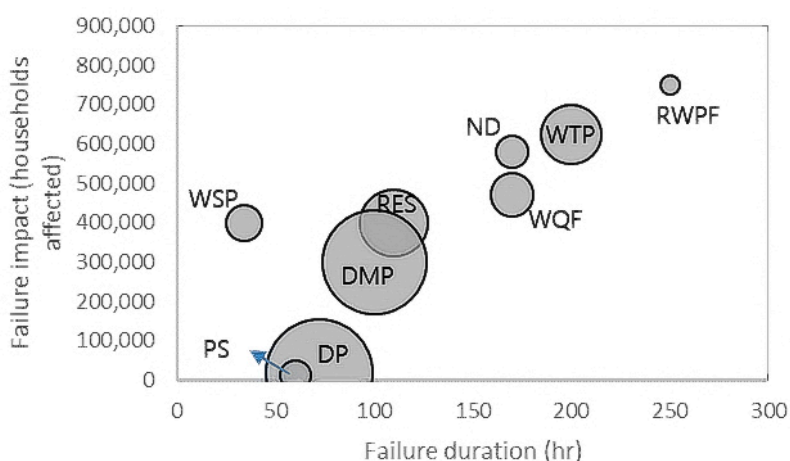


Figure 2. Example of the CID bubble plot.

Therefore, compared with the CID plot, the CID bubble plot provides rough information on failure duration and impact but has the advantage of providing relative failure frequency information.

3. Data

In order to verify the proposed CID and bubble plots, we collected the records of 331 WSDS component failures that occurred in South Korea between 1980 and 2018. Note that nation-wide failure data was collected and used to produce the plots because of data scarcity. Thus, the detailed description of the WSDS characteristics were not available. This is only for demonstration purposes, and one can use a single utility failure data, if sufficient, to create the plots suitable for site-specific decision-making tools.

Most water utilities in Korea stipulate filling out a failure event response sheet in which the date, cause, response action is taken, impact and duration (consequences), lessons, and figures should be recorded in the event of a component failure. It is worthwhile to highlight that the administration in South Korea generally records impact on the household unit (e.g., the number of households out of service) for simplicity purpose. The two largest water providers in Korea, the Office of Waterworks of Seoul Metropolitan Government (about 10 million customers) and K-water, regularly publish a WSDS failure casebook, i.e., the collection of the response sheets. In addition, the aforementioned failure cause and consequences information are often found in news articles, especially when the failure consequence is relatively significant. Therefore, this study used the historical failure data collected from the casebooks (1980–2015) and news articles (2008–2018).

Table 2 summarizes several statistics for the collected WSDS component failures. DP and DMP are the most common failures in WSDSs in Korea, covering 31.4 and 29.6% of the total 331 failures, respectively. The longest average and maximum failure durations (41 and 120 h, respectively) were RWPF failures. However, the maximum failure impact, which is the maximum number of households out of service, was observed in a WTP failure (0.623 million households). Note that the average number of persons in a household in Korea has remained steady at 2.5 since 2015. A more comprehensive and effective understanding of the failure data can be achieved with the proposed CID plots in the next section.

Table 2. Statistics of the historical water supply and distribution system (WSDS) component failures considered in this study.

Level-II Failure Categorization	Failure Duration (hr)			Failure Impact (hr)—The Number of Households Out of Service			Number of Failure Events (<i>n_j</i> in Equation (1))	Proportion (%)
	Min	Average	Max	Min	Average	Max		
RWPF	8	41	120	30,000	164,000	500,000	4	1.2
WTP	1	24.5	60	20	83,474	623,000	33	10.0
RES	4	7.7	11.5	70	41,495	282,864	10	3.0
PS	2	12	72	50	34,328	471,000	18	5.5
WSP	3	27	216	69	39,965	295,000	42	12.7
DMP	1	12	240	300	22,521	505,000	98	29.6
DP	1	7	72	2	1001	20,000	104	31.4
WQF	10	25	72	8	3664	12,000	9	2.7
ND	4	14	34	200	74,273	400,000	13	3.9
Total							331	100

4. Application Results

4.1. CID Plot

Two CID and nine ID plots were drawn using the 331 component failure records (Figures 3 and 4, respectively). The former is the CID plot with box subplots bounded by the minimum and maximum (Figure 3a, CID-1) and the average and maximum (Figure 3b, CID-2) of the duration and impact of nine WSDS failure triggers as classified in Table 1. A single 2-dimensional ID plot is drawn for each of the nine triggers with identical *x*- and *y*-axis (failure duration and impact, respectively) scales for effective comparison (Figure 4).

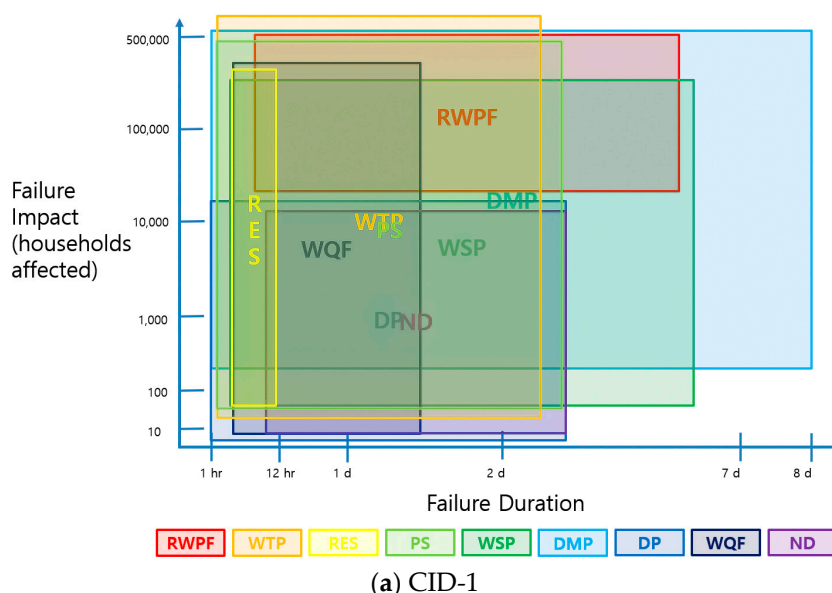


Figure 3. Cont.

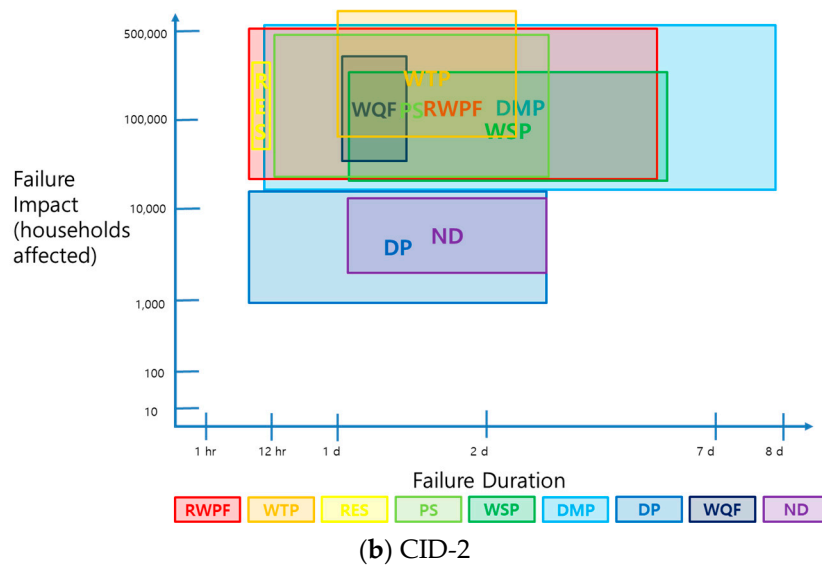


Figure 3. CID plots constructed from 331 component failure records bounded by (a) the minimum and maximum (CID-1 plot) and (b) the average and maximum (CID-2 plot) of the duration and impact of nine failures in Table 1.

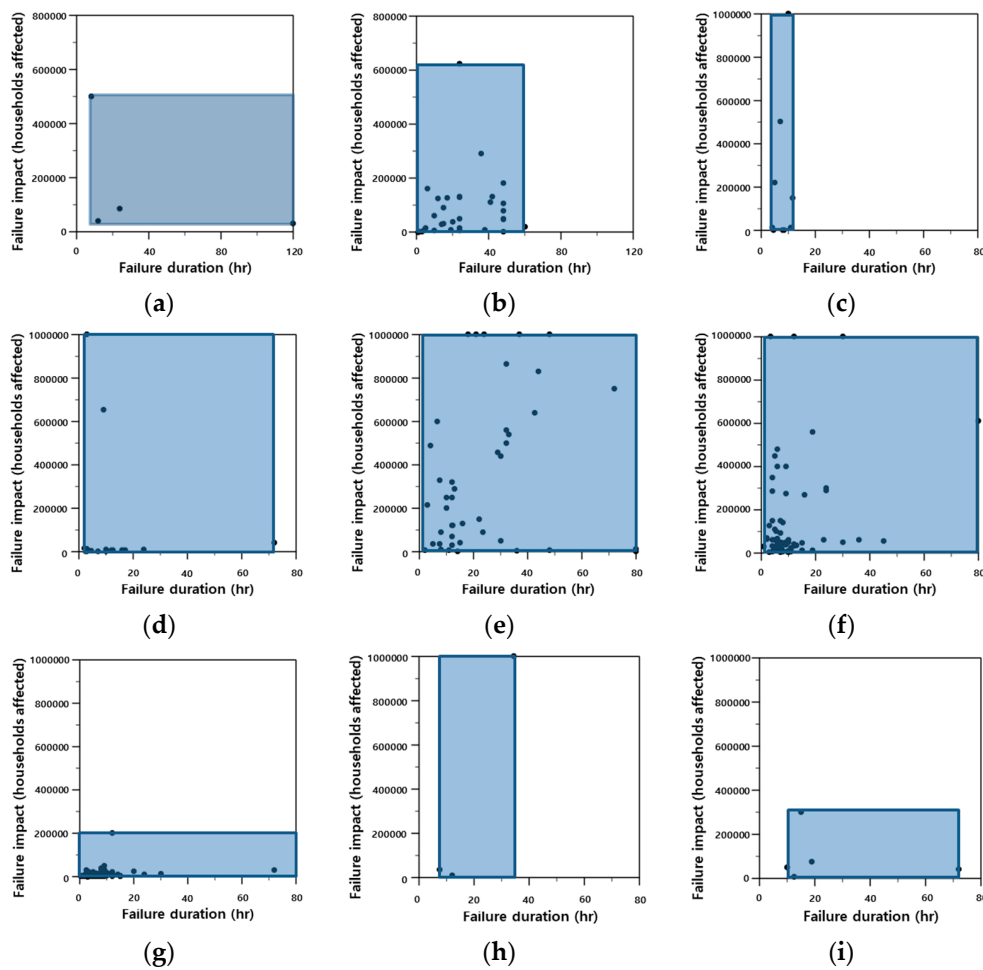


Figure 4. Individual impact–duration (ID) plots for different failures (failure duration in *x*-axis and failure impact in *y*-axis): (a) raw water pumping facility (RWPF), (b) water treatment plant (WTP), (c) reservoir (RES), (d) pump station (PS), (e) water supply pipe (WSP), (f) distribution main pipe (DMP), (g) distribution pipe (DP), (h) water quality failure (WQF), and (i) natural disaster (ND).

As shown in Figure 3a, the CID-1 plot has box subplots overlapping each other because each of the nine failure triggers has a wide range of failure duration and impact (Table 1). This is due to the use of nation-wide data in this study. Opposite to what would be expected, components located upstream of WSDS were not always positioned in the upper right corner of the CID plot (Q1) constructed from the 331 failures considered in this study. For example, the maximum failure duration of RES (approximately a half-day) was shorter than that of DMP (10 d), which resulted in a RES box with narrow width being positioned in the left corner of the CID-1 plot (Figure 3a), and a big DMP box covering every quadrant (Figure 3a). A better CID-1 plot would be obtained if a sufficient number of failure records collected in an individual city are used.

The CID-2 plot provides a better view of an individual failure's overall consequence range, as the coordinate of the left edge of each box is equal to the average failure duration, whereas that of the lower edge is the average number of households experiencing water service outage (Figure 3b). While the RES box shrunk toward Q2, the CID-2 plot clearly shows that the DP and ND failures were the most minor failures compared with other failures considered in this study, because their boxes are located near Q4. Generally, only a local district in the downstream of a broken DP would be isolated for recovery. Thirteen failure events classified as ND (external failure cause) were WSDS component failures directly from typhoons and flooding with insignificant failure consequences. It was clearly confirmed from CID-2 plot that the component failures by ND considered in this study were not critical ones. The operation of an emergency readiness team during the disasters would help limit any further increase in the failure consequences, but the box would expand toward Q1 if seismic failures were considered (i.e., multiple component failures) [12] (Figure 3b). Note that other boxes, e.g., RWPF, WTP, PS, WSP, WQF, also overlapped in the CID-2 plot.

While the two CID plots can serve as useful tools to identify the most minor and major component failures (with the historical records considered in this study), the individual ID plots can provide a firm platform for detailed failure consequence comparison between the nine failures (Figure 4). The nine individual ID plots not only present a bounded box area, but also contain the consequence data points of each failure category by which the point distribution could be identified. In this study, we use two different x - and y -axis scales to better display the distribution of the data points. The x - and y -axes for RWPF and WTP are consistently set to range from 0 to 120 h (10 d) and from 0 to 0.8 M households (e.g., the entire city), respectively (Figure 4a,b). Note that the ranges are 0 to 80 h (6.7 d) and from 0 to 0.1 M households for other components (Figure 4c–i). Data points beyond these ranges were assumed to be the maximum x and y -axis values (e.g., the maximum failure impact of DMP was 0.505 M households, Table 2), which was represented as 0.1 M households (the maximum y -axis value in Figure 5f). While some of the failures have few data points (Figure 4a,h,i), most of the box area (its width and height) was determined under the bias of a few extreme data points.

The shape of some of the boxes (i.e., the relative width and height) in the individual ID plots (Figure 4c,g,i) is similar to those included in the CID-2 plot (e.g., RES, DP, and ND boxes in Figure 3b). Most data points were gathered in the lower left corner of the WSP, DMP, and DP (i.e., pipe failures) ID plots (Figure 4e–g, respectively), indicating that the majority of the failure events were responded to and managed well. Therefore, water utility should focus on developing special strategies to promptly and effectively respond to few extreme failure events which cause a relatively long failure duration and great impact compared to other failures in the same category (Figure 4).

4.2. CID Bubble Plot

By using the failure data, two CID bubble plots were drawn: One with the center of the bubble positioned at the maximum (Figure 5a, ID-1), and the other with the center at the average value of the failure duration and impact (Figure 5b, ID-2). Because the bubbles are shifted toward the lower left corner of the CID plot in the latter case (the maximum is bigger than the average), the two bubble plots have different x - and y -axis scales for better visualization. Note again that the radius of each bubble is proportional to each failure's frequency and proportion (occurrence likelihood) in Table 2.

The most critical failure can be determined from the two ID plots based on the radius and location of the bubble: The bubble with a large radius (high occurrence likelihood) located in the upper right corner (Q1) indicates the most critical one (Figure 5). It was confirmed from the ID-1 plot that DMP and DP are the most frequent types of failures while the DMP also has the longest maximum failure duration (Figure 5a). However, the ID-2 plot indicates that their expected (average) failure consequences are smaller than other failures (Figure 5b). Based on the ID-2 plot, RWPF failure is the most critical failure but has a low likelihood because a small bubble is located in Q1. Note that only four failure events are of the RWPF type among the total 331 failures (1.2%) considered in this study (Table 2). Considering both ID plots, RWPF, WTP, WSP, and DMP are the critical components in WSDSs in Korea for which failure can cause significant consequences. It was verified that the CID bubble plots are useful for comparing and selecting WSDS component failures with respect to their failure consequences and occurrence likelihood.

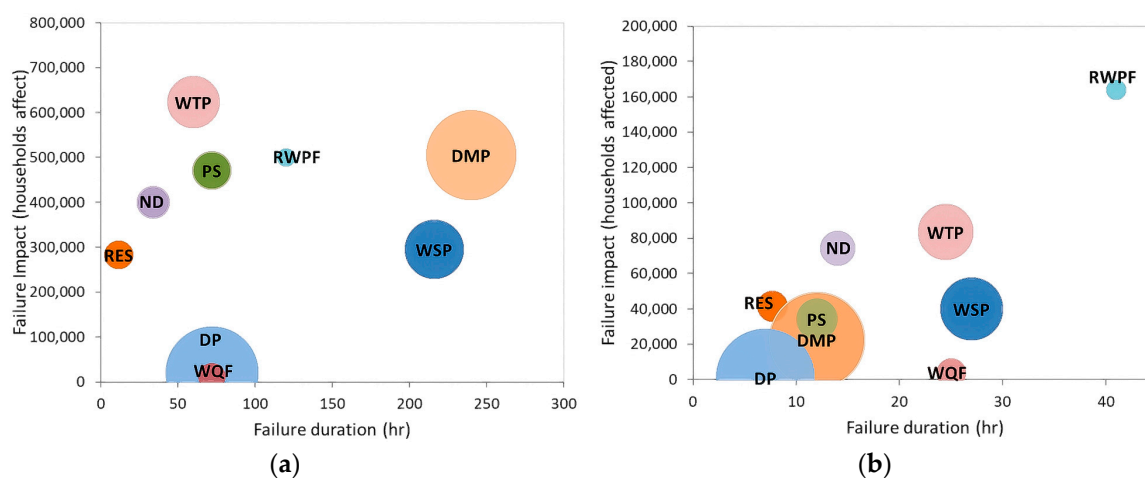


Figure 5. CID bubble plots with the center of the bubble positioned at (a) the maximum, and (b) the average value of the failure duration and impact. Their radius is proportional to the failure event's frequency in Table 2.

4.3. Broader Impact

The goal of CID visualization is to provide the management strategy of the WSDS intuitively. For the past few decades, resilient and robust planning has become an important consideration of the WSDS planning and management purpose owing to the high uncertainty of disturbances and the consequences of component failure [10,21]. Thus, knowing the variation (or uncertainty) of the failure consequences and preparing for the variation is of paramount importance for the utility and all other stakeholders to which both CID-1 and CID-2 plots (Figure 3) can deliver an important message for the purpose. First, CID-1 is not only showing how severe the consequence was of each failure trigger but also which trigger induces the most uncertain consequence; while CID-2 shows a similar vision but focusing on more severe events. For example, DMP in CID-1 shows a wide range of failure duration and impact, which indicate the need for a better isolation strategy or the installation of isolation valves to reduce the variation of the consequence. Moreover, the prioritization of management planning can be sought based on the location of each trigger, depending on the preference of the utility. For the given example in Figure 3a, and assuming the utility is more aware of significant failure (e.g., right upper corner of each rectangular), DMP, RWPF, and WSP will be the high priority of management. In other words, close scrutiny is required for DMP, RWPF, and WSP. On the other hand, if the utility only cares about the failure impact, then WTP, DMP, and RWPF will be the high priority of management. Thus, both CID plots can serve as a reference for resilient and robust WSDS planning and management. Regarding CID bubble plots (Figure 5), a similar conclusion is also derived by the size (radius) and the

location of the bubble. Additionally, CID bubble plots are showing the frequency of the failure as well, which is not shown in CID plots.

The individual ID plots shown in Figure 4 can also be expressed as a form of the response surface, which is a heat map-like graph reflecting data with different coloring. It has been frequently used for adaptation planning by visualizing the impact of climate change for decision making purposes [22,23]. Suggesting a response surface is not exactly same with the one used for those studies, but we can adapt the heatmap format to re-create the individual ID plots. However, for this type of visualization, more data is better since the color variation will be better illustrated. For this reason, only WSP, DMP, and DP ID response surface is illustrated in Figure 6.

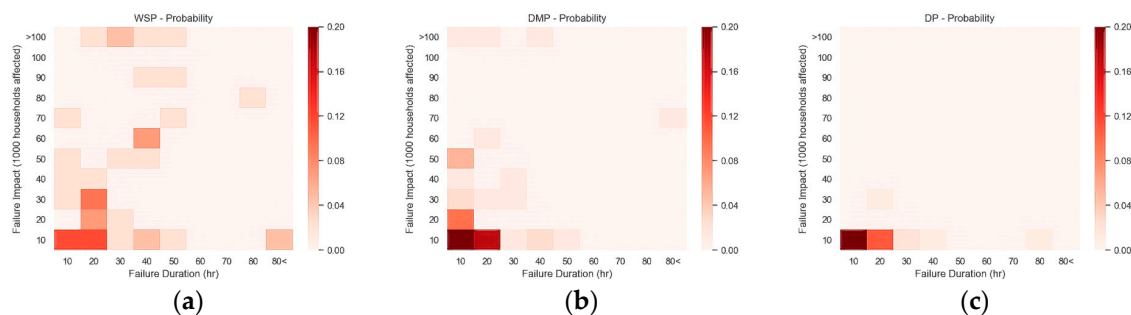


Figure 6. Individual ID response surface for different failures: (a) WSP, (b) DMP, and (c) DP.

As shown in Figure 6, the color changes as the probability of the given failure impact and duration changes. Note that darker color is a higher probability of occurrence. Figure 6 implies the same message as Figure 4 does, but enhances the visualization of Figure 4 if the sufficient amount of data can be acquired. In addition, since this type of visualization is frequently used for adaptation planning, this visualization approach can also provide the high probability of an event that utility should aware of or probability of high failure consequence. Especially providing probability of high failure consequence can help the utility to determine whether investment for the high failure consequence is worthwhile or not. Moreover, the quantified risk of each failure consequence can be provided if the probability can be fully investigated.

5. Summary and Conclusions

This study proposed CID and bubble plots to effectively display the relationship between the failure cause and consequences (duration and impact) of WSDSs and to help communicate with non-professional stakeholders (i.e., policymakers, practitioners, lawyers, etc.). The proposed CID plot provides an effective snapshot of the ranges (extents) of failure duration and the impact of different failures, whereas the CID bubble plot contains failure frequency information. This study also introduced a simple and practical failure classification system that categorized WSDS failure into nine component failures (RWPF, WTP, RES, PS, WSP, DMP, DP, WQF, and ND). To verify the proposed visualization methods, we produced the proposed plots using the historical records of 331 WSDS component failures, which were collected in South Korea from 1980 to 2018. DP and DMP were the most frequent failures in Korean WSDSs, comprising 31.4 and 29.6% of the total 331 failures, respectively.

First, two CID plots were drawn using the 331 failure records: (1) One with box subplots bounded by the maximum and minimum of the failure duration and impact, and (2) the other with subplots bounded by the average and maximum values. While most box subplots overlapped in the former, the latter plot clearly identified the most minor and major component failures. Then, nine individual ID plots were drawn, each of which showed the relationship between the failure duration and impact of an individual failure cause. It was confirmed from the ID plots that most of the box area (its width and height) was determined under the bias of a few extreme data points. The individual ID response surface is also suggested as an alternative form of the individual ID plot. Lastly, the CID bubble plots were produced with the center of the bubbles positioned at either the maximum or the average values

of the failure duration and impact. The radius of the bubble indicated the relative occurrence likelihood of corresponding failure. RWPF, WTP, WSP, and DMP were the most critical components in Korean WSDSs based on the bubble plots.

It was confirmed that (1) the CID plots can serve as a useful tool to identify the most minor and major WSDS failures, and (2) the bubble plots are useful in determining the most significant failures with respect to their failure consequences and occurrence likelihoods. Collecting a sufficient number of historical failure records for various components will help in constructing more reliable CID and bubble plots.

This study has several limitations that future research must address. First, we collected records for component failures that occurred across multiple WSDSs in Korea. A water utility may want to limit their data collection to failures that occurred in their WSDS to have a system-specific relationship between failure cause and consequences. To that end, a sufficient number of failure records should be collected, with each failure event classified following the proposed classification system, and the failure duration and impact data properly documented. In the worst case, an estimation of the information should be recorded. Second, the proposed CID and bubble plots can be developed and compared under various WSDS conditions and characteristics. For example, it is worthwhile to compare plots with and without emergency pipes between district metering areas. Third, a 3-dimensional version of the CID and bubble plots could be constructed by displaying the temporal changes of the duration and impact over months/years along the z-axis. By indicating the major changes in WSDSs (e.g., parallel pipe construction in WSP lines, development of industrial complex in part of the system) in the z-axis (with arrow and text), these plots will effectively show the transition of the failure consequences upon system condition changes. Lastly, probability can be assigned to the CID plots to guide the water utility to conduct a risk analysis. The quantified risk of failure impact and duration can also be calculated once the probability is fully established.

Author Contributions: S.O. and H.J. equivalently contributed to the literature review and summary, data collection and analysis, and CID and bubble plot development and generation. D.J. and S.L. contributed to manuscript writing and the recommendation of potential research topics.

Funding: This subject was supported by Korea Ministry of Environment as “Global Top Project (2016002120003).”

Conflicts of Interest: The authors declare no conflict of interest.

References

1. Jung, D.; Yoo, D.G.; Kang, D.; Kim, J.H. Linear Model for Estimating Water Distribution System Reliability. *J. Water Resour. Plan. Manag.* **2016**, *142*, 4016022. [[CrossRef](#)]
2. Lansley, K. Sustainable, robust, resilient, water distribution systems. In Proceedings of the WDSA 2012: 14th Water Distribution Systems Analysis Conference, Adelaide, South Australia, 24–27 September 2012; p. 1.
3. Lee, S.; Shin, S.; Judi, D.R.; McPherson, T.; Burian, S.J. Criticality Analysis of a Water Distribution System Considering Both Economic Consequences and Hydraulic Loss Using Modern Portfolio Theory. *Water* **2019**, *11*, 1222. [[CrossRef](#)]
4. PieTrucha-urbaniK, K.; Studziński, A. Case study of failure simulation of pipelines conducted in chosen water supply system. *Ekspluat. Niezawodn.* **2017**, *19*. [[CrossRef](#)]
5. Jun, H.; Loganathan, G.V. Valve-Controlled Segments in Water Distribution Systems. *J. Water Resour. Plan. Manag.* **2007**, *133*, 145–155. [[CrossRef](#)]
6. Creaco, E.; Franchini, M.; Alvisi, S. Evaluating Water Demand Shortfalls in Segment Analysis. *Water Resour. Manag.* **2012**, *26*, 2301–2321. [[CrossRef](#)]
7. Oak, S.; Kim, S.; Jun, H. An application of the A-PDA model and the water supply performance index for the temporal and spatial evaluation of the performance of emergency water supply plans via interconnections. *J. Korea Water Resour. Assoc.* **2018**, *51*, 977–987.
8. Martini, A.; Rivola, A.; Troncosi, M. Autocorrelation Analysis of Vibro-Acoustic Signals Measured in a Test Field for Water Leak Detection. *Appl. Sci.* **2018**, *8*, 2450. [[CrossRef](#)]

9. Nayak, M.A.; Turnquist, M.A. Optimal Recovery from Disruptions in Water Distribution Networks. *Comput. Civ. Infrastruct. Eng.* **2016**, *31*, 566–579. [[CrossRef](#)]
10. Shin, S.; Lee, S.; Judi, D.R.; Parvania, M.; Goharian, E.; McPherson, T.; Burian, S.J. A Systematic Review of Quantitative Resilience Measures for Water Infrastructure Systems. *Water* **2018**, *10*, 164. [[CrossRef](#)]
11. Yazdekhashti, S.; Piratla, K.R.; Atamturktur, S.; Khan, A. Experimental evaluation of a vibration-based leak detection technique for water pipelines. *Struct. Infrastruct. Eng.* **2018**, *14*, 46–55. [[CrossRef](#)]
12. Farmani, R.; Kakoudakis, K.; Behzadian, K.; Butler, D. Pipe Failure Prediction in Water Distribution Systems Considering Static and Dynamic Factors. *Procedia Eng.* **2017**, *186*, 117–126. [[CrossRef](#)]
13. Tabesh, M.; Soltani, J.; Farmani, R.; Savic, D. Assessing pipe failure rate and mechanical reliability of water distribution networks using data-driven modeling. *J. Hydroinforma.* **2009**, *11*, 1–17. [[CrossRef](#)]
14. Onyango, L.A.; Quinn, C.; Tng, K.H.; Wood, J.G.; Leslie, G. A Study of Failure Events in Drinking Water Systems as a Basis for Comparison and Evaluation of the Efficacy of Potable Reuse Schemes. *Environ. Health Insights (EHI)* **2015**, *9*, S31749. [[CrossRef](#)]
15. Lindhe, A.; Rosén, L.; Norberg, T.; Bergstedt, O. Fault tree analysis for integrated and probabilistic risk analysis of drinking water systems. *Water Res.* **2009**, *43*, 1641–1653. [[CrossRef](#)]
16. Rak, J.R.; Pietrucha-Urbanik, K. An Approach to Determine Risk Indices for Drinking Water—Study Investigation. *Sustainability* **2019**, *11*, 3189. [[CrossRef](#)]
17. Fletcher, S.M.; Miotti, M.; Swaminathan, J.; Klemun, M.M.; Strzepek, K.; Siddiqi, A. Water Supply Infrastructure Planning: Decision-Making Framework to Classify Multiple Uncertainties and Evaluate Flexible Design. *J. Water Resour. Plan. Manag.* **2017**, *143*, 4017061. [[CrossRef](#)]
18. Folkman, S. *Water Main Break rates in the USA and Canada: A Comprehensive Study*; Mechanical and Aerospace Engineering Faculty Publications, Utah State University: Logan, UT, USA, 2018.
19. Clark, R.M.; Thurnau, R.C. Evaluating the Risks of Water Distribution System Failure. *Opflow* **2011**, *37*, 24–28. [[CrossRef](#)]
20. Zhang, X.; Mi, Z.; Wang, Y.; Liu, S.; Niu, Z.; Lu, P.; Wang, J.; Gu, J.; Chen, C. A red water occurrence in drinking water distribution systems caused by changes in water source in Beijing, China: Mechanism analysis and control measures. *Front. Environ. Sci. Eng.* **2014**, *8*, 417–426. [[CrossRef](#)]
21. Jung, D.; Lee, S.; Kim, J.H. Robustness and Water Distribution System: State-of-the-Art Review. *Water* **2019**, *11*, 974. [[CrossRef](#)]
22. Brown, C.; Ghile, Y.; Laverty, M.; Li, K. Decision scaling: Linking bottom-up vulnerability analysis with climate projections in the water sector. *Water Resour. Res.* **2012**, *48*, 48. [[CrossRef](#)]
23. Kay, A.; Crooks, S.; Reynard, N. Using response surfaces to estimate impacts of climate change on flood peaks: Assessment of uncertainty. *Hydrol. Process.* **2014**, *28*, 5273–5287. [[CrossRef](#)]

